Wall-correction and absorbed-dose conversion factors for Fricke dosimetry: Monte Carlo calculations and measurements

Chang-ming Ma[a)]
Physics Department, Institute of Cancer Research and Royal Marsden Hospital, Sutton, Surrey, United Kingdom

D. W. O. Rogers, K. R. Shortt, and C. K. Ross
Ionizing Radiation Standards, Institute for National Measurement Standards, National Research Council Canada, Ottawa K1A 0R6, Canada

A. E. Nahum
Physics Department, Institute of Cancer Research and Royal Marsden Hospital, Sutton, Surrey, United Kingdom

A. F. Bielajew
Ionizing Radiation Standards, Institute for National Measurement Standards, National Research Council Canada, Ottawa K1A 0R6, Canada

(Received 26 October 1992; accepted for publication 10 December 1992)

For megavoltage radiotherapy photon beams, EGS4 Monte Carlo calculations show, and experimental measurements confirm with an accuracy of 0.2%, that glass or quartz-walled vials used in Fricke dosimetry increase the dose in the Fricke solution. This is mainly caused by increased electron scattering from the glass which increases the dose to the Fricke solution. The dose perturbation is shown to vary from nothing in a ^{60}Co beam up to 2% in a 24-MV beam. For plastic vials of similar shapes, calculations demonstrate that the effect is in the opposite direction and even at high energies it is much less (0.2% to 0.5%).

I. INTRODUCTION

The Fricke ferrous sulphate dosimeter is recognized to be the most suitable chemical system available for radiation dosimetry with respect to accuracy, reproducibility, and linearity of response. It is relatively independent of the dose rate and of radiation quality.[1-3] Its composition is close to that of water and therefore only introduces a small perturbation in the radiation field if the dosimeter vessels are also made of materials with properties similar to water. Both the AAPM and ICRU have recommended the use of Fricke dosimetry as an alternative method for the calibration and the determination of absorbed dose in water.[4,2] Several primary standards dosimetry laboratories are using Fricke dosimetry either as part of a primary standard for absorbed dose to water [National Research Council Canada (NRC), Physikalische Technische Bundesanstalt of Germany (PTB)] or as part of a calibration service for clinical accelerators [National Physical Laboratory, UK (NPL), National Institute for Standards and Technology, USA (NIST)].

ICRU Report 35[2] recommended the use of plastic dosimeter vessels for Fricke dosimetry in the determination of absorbed dose in a phantom irradiated by high-energy photon and electron beams. Plastic vessels have linear attenuation coefficients and stopping-power values somewhat less than those for water, and this compensates for the somewhat greater values in the ferrous sulphate solution. The main purpose of using plastic vessels is to minimize the perturbation effects on the electron scattering introduced by the presence of the Fricke dosimeter in the water phantom.[5] However, a great deal of care is required with plastic vessels because of storage effects, i.e., chemical effects on the ferrous sulphate solution when stored in the plastic container.[6] Glass irradiation vessels can be cleaned so that there is no storage effect.[7] They are therefore the vessels of choice when there is a delay before read out, for example in intercomparison experiments or calibration services. For these glass vessels, the perturbation and cavity theory effects are potentially large.[2] Burlin and Chan showed both experimentally and theoretically that the cavity theory effects could be as large as 7% with small volumes of Fricke solution in thick-walled silica vessels in a ^{60}Co beam.[8] This is because in the normal, i.e., large volume detector, one considers the Fricke solution to be a photon detector in which all the dose is delivered by electrons starting in the Fricke solution and hence $D_{\text{med}} = D_f\,(\overline{\mu_{\text{en}}/\rho})^{\text{med}}_{\text{Fricke}}$ where D_{med} is the dose to the medium and D_f is the dose to the Fricke solution. However, in the small volume detector one has an electron detector in which the dose is delivered by electrons starting in the walls and hence Bragg–Gray cavity theory applies and one has $D_{\text{med}} = D_f(\bar{L}/\rho)^{\text{wall}}_{\text{Fricke}}(\overline{\mu_{\text{en}}/\rho})^{\text{med}}_{\text{wall}}$. The real situation is somewhere in-between these two extremes and Burlin and Chan applied a general cavity theory to the ^{60}Co case.[8] Ma and Nahum have extended the theory to the more complex case in which electrons from the medium are also detected in the Fricke solution.[9] Their Monte Carlo calculations of the wall-correction factor for Fricke dosimetry for high-energy photon beams show that for a 1-mm-thick pyrex-walled vial which is 5.7 cm long by 1.5 cm in diameter, the correction for the wall not being water equivalent varies from 1.00 for a ^{60}Co beam to 0.983 ± 0.001 for a 24-MV beam. These results explain the experiments reported by

Kwa and Kornelsen[10] although Kwa and Kornelsen interpreted their observations differently.

The scope of this study is to investigate Fricke-to-water dose conversion factors and wall-correction factors for high-energy photon beams for the fused-quartz-walled coin-shaped Fricke ferrous sulphate detectors used by the NRC and for the glass-walled small bottle-shaped vials used by the NPL and PTB. The effect of using different wall materials is investigated and a series of high-precision experiments is reported in which the difference in Fricke dose measured with quartz-walled and polyethylene-walled vessels is compared to the Monte Carlo predictions. Another series of experiments and calculations of the dose perturbations near quartz walls in a 20-MV photon beam is presented. These perturbations indicate that electron scattering from the quartz vials is the principle contributor to the overall effect of the wall.

II. DEFINITIONS OF CORRECTION FACTORS

Notation is discussed more fully elsewhere.[9] In this paper, D_f denotes the absorbed dose to the dosimeter solution when irradiated at depth in a water phantom. For high-energy photon beams the absorbed dose to water averaged over the volume occupied by the dosimeter solution is denoted by D_w and is given by:

$$D_w = f\, p_{\text{wall}} D_f \text{ (Gy)}, \tag{1}$$

where f is the absorbed-dose conversion factor which converts the dose to Fricke solution in a wall-less vessel to dose to water in the same location and p_{wall} is the wall-correction factor which accounts for the change in the absorbed dose in the Fricke solution due to the presence of wall material which is not water equivalent.

III. MONTE CARLO CALCULATIONS

A. The code DOSIMETER

The Monte Carlo calculations were done with the EGS4[11] user-code DOSIMETER which is described in detail elsewhere.[9,12] Briefly, it is an extension of the NRC user-code CAVRZ[13–15] for calculating ion chamber response. It uses the PRESTA algorithm[16] and ICRU Report 37 stopping powers.[17] The major changes are: (1) circular or rectangular fields incident on a cubic phantom can be used and the ion chamber can have its axis perpendicular or parallel to the surface; (2) to reduce variance, a correlated sampling technique is used which only follows separately those parts of a photon shower after entry into regions in which the materials vary; and (3) the code scores separately the dose from photon interactions in the medium, wall and detector materials.

In all cases, uniform circular or rectangular beams, 100 cm^2 in area were incident perpendicular to the surface of a water phantom. Variations in beam spectra across the beam were ignored. The detectors were assumed to have their central axis at the depth of measurement which was taken as 7 cm for beams of 20 MV and above and 5 cm at lower energies.

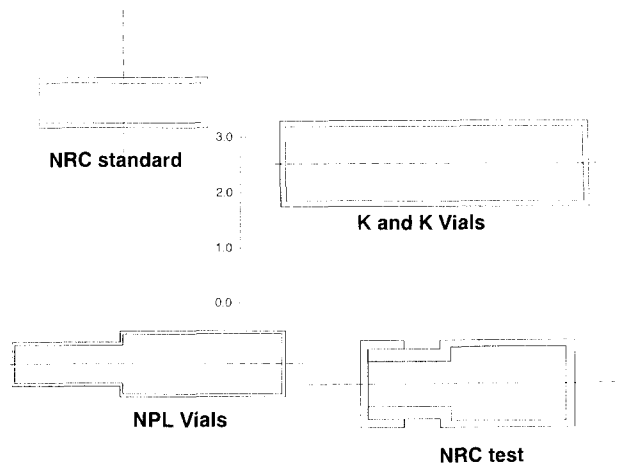

FIG. 1. Scale cross-sectional drawings of the vials as modeled in this study. The scale shown is in cm. All vials are cylindrical and the dashed lines are the axes of rotation. In all cases, the beam is from above and incident on a flat face of the phantom above the vials (although in the experiments the beam was horizontal). The vials were centered at 5 cm for beams with $TPR_{10}^{20} < 0.75$ and at 7-cm depth for higher energy beams.

The calculations were done on a silicon graphics Irix/240 server with 4 to 8 cpus, each 13 times faster than a VAX 11/780. Runs took from 60 h up to 300 h of cpu time in the worst case.

B. The vials

Calculations have been done for a wide variety of vials. In all cases the vials have been modeled as closely as possible using the cylindrical geometry package available in the code DOSIMETER. Figure 1 shows scale cross-sectional views of the vials considered in this study. The beam enters from the top of the figure in all cases. Calculations were done for a variety of wall materials including pyrex glass, PMMA, polyethylene, and polystyrene. In subsidiary calculations we have shown that there is no difference in calculated p_{wall} values between modeling the walls as fused quartz or pyrex-glass (the mass-energy absorption coefficients and mass stopping powers differ by much less than 1%). Details of the vial dimensions are given in the appendix. Note that the NPL vials have walls which are roughly half as thick as for each of the other vial types. In several cases the possibility of air bubbles in the vials were included in the calculations.

C. Spectra used

The calculations all require knowledge of the incident photon spectrum. For the ^{60}Co beam a spectrum was used which included a 30% fluence contribution from photons scattered from the source capsule and collimators.[18] For typical clinical spectra, the widely utilized calculated spectra of Mohan *et al.* were used.[19] Calculations were also done for two photon beams at 10 and 20 MV which are used for standards work at NRC. They are generated by electrons incident on a thick target of aluminum and each flattened by different conical aluminum flattening filters.

The last two beams were 30- and 50-MV beams from the Scanditronix 50-MV racetrack microtron in which bremsstrahlung beams from a thick tungsten/copper target are swept across the field to achieve flatness. For these last four spectra, preliminary EGS4-calculated on-axis photon spectra were obtained from the NRC user-code ACCEL which models cylindrically symmetric accelerator heads (this is a minor modification of the NRC user-code FLURZ described in detail in Ref. 20). The flattening filters were modeled as a stacked set of cylinders. The details of these calculations are not critical and the spectra are only used as representative of different spectra. The beam quality is specified by calculating[21] the value of TPR_{10}^{20} (Ref. 4) for these spectra based on the assumption that the spectra are uniform across the beam. To obtain the calculated corrections in any particular beam, the measured value of TPR_{10}^{20} should be used to interpolate the values presented below.

D. Checks of the code

Validation of the EGS4 Monte Carlo system has been extensively reviewed in the literature (see e.g., Ref. 22 and references therein). The user-code DOSIMETER and its use of correlated sampling are very complex. As one straightforward check of its accuracy, similar calculations were done using DOSRZ, a heavily used NRC user-code for scoring energy deposition in a cylindrical geometry. The 20-MV NRC photon beam was incident on the standard NRC quartz-walled vials at 7-cm depth and on a wall-less detector at the same point. The difference in the energy deposition in the Fricke solution was found to be $(1.64 \pm 0.14)\%$. This compares to a value of $(1.41 \pm 0.10)\%$ found for the same geometry using the code DOSIMETER. These results agree within the statistical uncertainties (1 s.d.).

To check for possible electron step-size effects, calculations were done using both the default PRESTA algorithm and using a maximum electron step-size of 1% energy loss per step. The cases considered were for the ^{60}Co spectrum and all the Mohan *et al.* spectra incident on the standard NRC vials in a phantom. The results of both sets of calculations agreed within the typical statistical precision of 0.1%. This demonstrates that there is no significant step-size effect and hence the default PRESTA algorithm has been used since it is roughly three times faster than the 1% ESTEPE calculations.

IV. NEW MEASUREMENTS

Two sets of measurements have been done using the NRC linear accelerator and ^{60}Co beam.

A. Ratio of doses with different vials

Fricke dosimetry plays an essential role in the water calorimeter-based absorbed-dose standards being developed at NRC.[23,24] It is also the basis of a clinical calibration service which requires storage of vials before reading and hence quartz-walled vials have been used. The practice of Fricke dosimetry at NRC is described in the references. The essential feature to note is that a measurement precision of 0.1% to 0.2% is routinely available.

The present experiment consisted of measuring the absorbed dose in three different photon beams (^{60}Co, 10 MV and 20 MV) using two different types of Fricke dosimeter vials—one with 1-mm fused quartz walls (the standard NRC vial—see the appendix), the other with 1.6-mm polyethylene walls. When using the two types of vials, the ratio of the measured response per unit dose in a given beam can be compared to the ratio of the calculated correction factors.

The experiments with the polyethylene walled detectors were somewhat less precise than usually obtained with the quartz vials, probably because of contact between the Fricke solution and the plastic. Nonetheless an overall uncertainty of 0.2% (1σ) was achieved. Each data point represents the average result for three irradiation sessions for the ^{60}Co and 20-MV beams and two sessions for the 10-MV beam. During each session at least five vials of each type were irradiated.

B. Diode measurements near quartz containers

To elucidate the mechanisms involved in the wall perturbations, a series of dose measurements around quartz vials in a water phantom have been done using a small diode detector developed at NRC. The detector is about 1 mm on each side and has been mounted so as to have an isotropic response. Its output has been shown to be proportional to absorbed dose in electron beams by comparison to calibrated parallel plate ion chambers[25] and is assumed to measure dose accurately in the current experiments as well.

Measurements relative to the dose in a homogeneous water phantom have been performed. In one set of measurements the dose was measured as a function of radial position relative to the central axis of the vial, in planes 0.4, 1, and 2-mm upstream of the standard NRC vials. In a similar set of measurements the relative dose was measured in a plane immediately behind the vials as a function of radial position. In a third set of measurements the relative dose beside the vials was measured as a function of the depth downstream from the front of the vial at several radial distances outside the vial (0.4, 2, and 4 mm).

The dose perturbations were usually of the order of a few percent at most and varied rapidly near the vials. This required careful alignment to be done. Because the measurements done were relative, considerable detail was obtained in the measurements.

V. RESULTS AND DISCUSSION

A. Absorbed-dose conversion factors

Results for the calculated absorbed-dose conversion factors relating the absorbed dose in the Fricke solution to the absorbed dose in the homogeneous water phantom at the same point are presented in Table I and Fig. 2.

In principle this factor is a function of detector geometry and beam energy. However, the values of f are all consistent with 1.003. The constancy with beam quality is

TABLE I. Absorbed-dose conversion factors, f, for converting dose to Fricke solution into dose to water for Fricke vials of various shapes as described in the text. One standard deviation (1 s.d.) statistical uncertainties in the last digit are shown in brackets.

		NRC			
Beam	TPR_{10}^{20}	Standard	test	NPL	K&K
^{60}Co	0.58	1.0032(4)	1.0041(8)	1.0022(5)	1.0033(5)
4 MV	0.624	1.0030(4)		1.0031(7)	1.0037(6)
6 MV	0.667	1.0033(6)		1.0026(13)	1.0034(5)
10-MV NRC	0.699	1.0021(8)	1.0026(8)		
10 MV	0.731	1.0034(9)		1.0026(15)	1.0043(8)
15 MV	0.761	1.0035(10)		1.0027(15)	1.0041(7)
20-MV NRC	0.768	1.0023(5)	1.0021(10)		
30-MV RTM	0.794	1.0034(11)			
24 MV	0.804	1.0029(7)	1.0040(15)	1.0034(5)	1.0025(8)
50-MV RTM	0.848	1.0028(11)			

due to a fortuitous cancellation between changes in ratios of spectrum-averaged Fricke-to-water mass energy-absorption coefficients and collision stopping-power ratios as the Fricke detectors change from being primarily photon detectors at ^{60}Co energies (about 87% of the dose to the Fricke solution is from photon interactions in the detector material) to being primarily electron detectors at high energies (about 75% of the dose to the Fricke comes from electrons set in motion in the walls and surrounding medium at 24 MV). This is discussed at length elsewhere[9,26] and is mainly a Burlin cavity theory effect. Thus when all electron multiple scattering is turned off in the Monte Carlo calculations, the calculated values of f remain unchanged.

B. Wall-correction factors for NRC vials

1. NRC standard vials

Figure 3 and Table II present summaries of the calculated wall-correction factors p_{wall} for the standard coin-shaped, quartz-walled Fricke vials used at NRC. The most important point is that these corrections are substantial and must be taken into account. To facilitate their use these data have been fit to a simple linear expression in terms of TPR_{10}^{20}:

$$p_{wall} = 1.0478 - 0.08223(TPR_{10}^{20}). \quad (2)$$

The data show an apparent departure from a linear relationship near $TPR_{10}^{20} = 0.76$. This may be associated with the change in the reference depth from 5 to 7 cm at this point, or it may indicate that TPR_{10}^{20} is not a good beam quality indicator for this correction[27] or it may just be a statistical fluctuation. In any event, it is a small effect and will be ignored for the time being.

2. Measurements with other vials at NRC

Measurements have been done in three photon beams at NRC using the standard NRC quartz-walled vials and using the test vials with polyethylene walls. Figure 3 and Table II show that the calculated p_{wall} correction factors

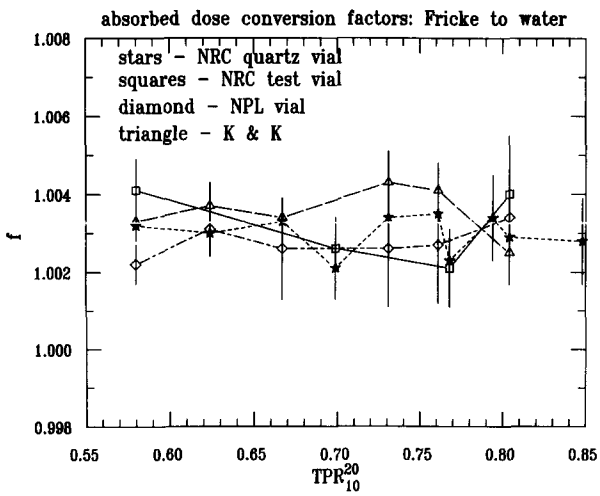

FIG. 2. Absorbed-dose conversion factors, f, for converting dose to Fricke solution into dose to water for Fricke vials of various shapes as described in the text. Stars, NRC standard vial shape; squares, NRC test vial shape; diamonds, NPL vial shape with no air gaps; triangles, long circular vial shape to model Kwa and Kornelsen vials.

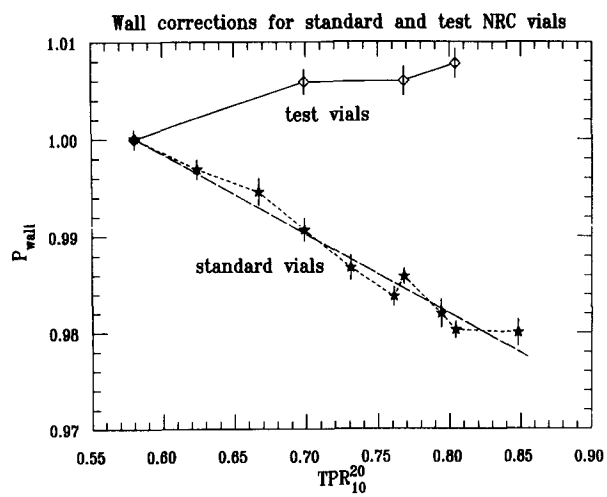

FIG. 3. Wall-correction factors, p_{wall}, for converting absorbed dose to Fricke solution measured in the standard quartz-walled vials and the polyethylene-walled test vials to dose in wall-less detectors. The dashed line shows the values from Eq. (2).

TABLE II. Wall-correction factors, p_{wall}, for converting absorbed-dose to Fricke solution measured in NRC vials to Fricke dose in wall-less detectors. Vials are placed on the central axis in uniform beams of 100 cm^2. They are centered at 5-cm depth for 15 MV and lower energy beams and at 7-cm depth at higher energies.

		p_{wall}	
Beam	TPR_{10}^{20}	Standard vial pyrex	test vial polyethelene
^{60}Co	0.58	1.0001(5)	1.0006(9)
4 MV	0.624	0.9969(10)	
6 MV	0.667	0.9946(14)	
10-MV NRC	0.699	0.9907(12)	1.0059(13)
10 MV	0.731	0.9868(13)	
15 MV	0.761	0.9838(10)	
20-MV NRC	0.768	0.9859(8)	1.0060(15)
30-MV RTM	0.794	0.9820(15)	
24 MV	0.804	0.9803(9)	1.0078(15)
50-MV RTM	0.848	0.9800(14)	

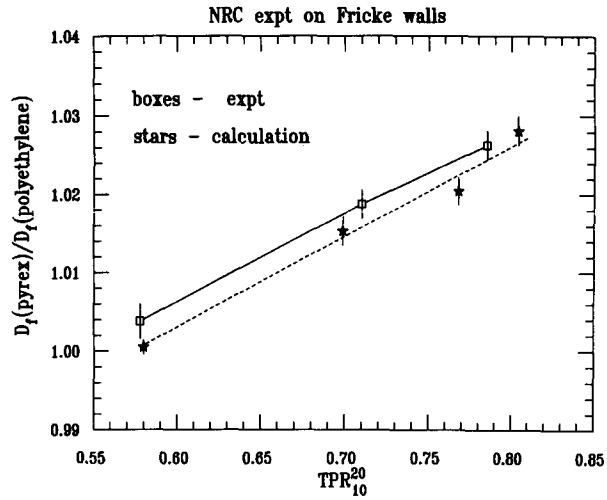

FIG. 4. Comparison of the measured and calculated ratio of the dose to Fricke solution in the standard quartz-walled vials to that in the polyethylene-walled test detector for various photon beam qualities. The dotted line is a least squares fit to the calculated data.

for the polyethylene-walled test vials are in the other direction compared to the case with quartz-walled standard vials, i.e., the polyethylene walls reduce the dose to the Fricke solution. Table I shows that the absorbed-dose conversion factors, f, are the same for both vials at all energies to within the 0.1% precision of the calculations and thus the ratio of the doses to the Fricke solution measured in the same beam at the same point should be the ratio of the predicted wall-correction factors for the two vials. These calculated and measured ratios are shown in Fig. 4. The agreement between the two is within 0.2%, the measured ratio being somewhat higher which may suggest a slight chemical effect which decreases the dose reading in the polyethylene-walled vial or some other systematic error in the experiment or calculations. For example, including the f factor in the comparison despite the fact that the differences in f for the two vials are statistically insignificant, would reduce the discrepancies by about 0.1% except in the 20-MV beam. Another possible source of error is the small air bubbles at the top of the polyethylene-walled vials. If the top 3 mm were considered filled with air then the calculated p_{wall} values would increase by up to 0.1% ($\pm 0.15\%$). This again improves the agreement with the experimental values—but it is not statistically significant and already represents a worst case estimate of the size of any air bubbles. Nonetheless, the agreement with the measurements at the 0.2% level is dramatic confirmation of the accuracy of the calculations.

3. Coin-shaped vials of other materials

The NRC vials are made of quartz because they were designed for use in a calibration service in which the vials were shipped to the clinic for measurements and hence must not suffer from chemical storage effects. However, in view of the correction factors found here, it may be more appropriate in-house to use plastic-walled vials. Hence calculations have been done for vials with the same dimensions as the standard vials, but with walls made of polystyrene, PMMA, and polyethylene. Figure 5 presents these calculated wall corrections and it is clear that they are much smaller than with pyrex walls. In particular, note that the calculated wall-correction factors for PMMA walls are less than 0.2% for TPR_{10}^{20} values less than 0.78. These vials are similar to those used by Mattsson *et al.*[5] who astutely selected this wall material to minimize wall effects.

C. Wall-correction factors for NPL vials

1. Calculated results

Table III and Fig. 6 present the calculated correction factors for the NPL vials. In this case the calculated effects are about half as large as with the standard NRC vials, presumably because the NPL vials have walls which are only half as thick. Table III also includes the calculated values of p_{air}, a correction which multiplies p_{wall} in order to take into account the air in the top portion of the NPL vial. The effect is of the order of 0.1% to 0.3%. The statistical uncertainty estimate shown for p_{air} is for the product of the overall correction factor, $p_{wall}p_{air}$ which is shown in Fig. 6 with p_{air}. When these vials are used at the PTB, they are sometimes held in a manner which includes air gaps and other materials outside the vials and at the NPL there is a plastic stand. In principle these non-water regions must also be taken into account. This has not been done in this work.

2. Comparison to experiment

Extensive comparisons have been done at the NPL between various methods of calibrating ion chambers in accelerator beams.[28] In one approach the absorbed-dose calibration factor has been determined as a function of beam quality using Fricke dosimetry as the basis of the measurements in beams other than ^{60}Co. For these same ion chambers they have calculated the absorbed-dose calibration factor using the standard HPA Protocol values of C_λ[29] which agree within 0.4% with the "best" estimates given in

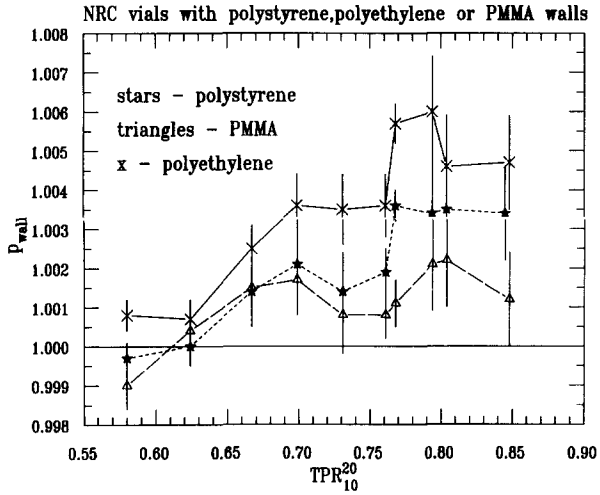

FIG. 5. Calculated wall-correction factors, p_{wall}, for Fricke vials with the dimensions of the standard NRC vials but with walls made of PMMA (triangles), polyethelene (crosses) and polystyrene (stars).

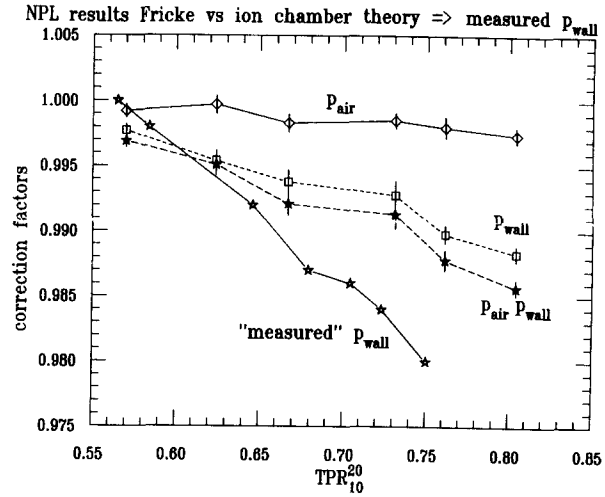

FIG. 6. Comparison of calculated and "measured" wall-correction factors, p_{wall}, for NPL Fricke vials. The measured values are shown by the solid line with stars, the calculations including the effect of an air bubble are given by stars with a dashed line and excluding the air bubble effects by the squares. The measured results are based on comparisons of ion chamber dosimetry using a dosimetry protocol and the dose assigned using an NPL Fricke dosimeter (which ignores p_{wall} effects and assumes ϵG is a constant for all the beam qualities considered) and are arbitrarily normalized to unity for ^{60}Co beams. The upper curve presents p_{air}, the calculated correction factor to take into account the air bubble in the top of the NPL vial.

references.[30,31] There are puzzling differences between the results obtained using different approaches. These differences can be at least partially explained by taking into account the wall-correction factors which were previously ignored in the NPL calibrations. Thus, using the Fricke-based absorbed-dose calibration factors $N_{D,\text{Fricke}}$ which were determined without correcting for p_{wall} effects, one must write:

$$D_{med} = M N_{D,\text{Fricke}} p_{wall}, \tag{3}$$

and one also has,

$$D_{med} = M N_{D,ion}, \tag{4}$$

where M is the corrected ion chamber reading in beams of different beam qualities. To eliminate any problems because the two systems are based on the use of different primary standards, we assume $p_{wall} = 1.0$ for ^{60}Co beams and hence for a beam quality Q:

$$p_{wall}(Q) = \frac{N_{D,ion}(Q) N_{D,\text{Fricke}}(^{60}\text{Co})}{N_{D,\text{Fricke}}(Q) N_{D,ion}(^{60}\text{Co})}. \tag{5}$$

Taking $N_{D,ion}$ from column 7 of table 4.5 in Ref. 28 and $N_{D,\text{Fricke}}$ from Figure 4.3 of the same report gives the values of p_{wall} implied by the NPL measurements (with an arbitrary normalization to unity at ^{60}Co). These are shown in Fig. 6 and compared to our Monte Carlo calculated values. The NPL Fricke results assume ϵG is a constant for all beam qualities. The much larger "measured" relative effects show that either the Monte Carlo calculated values are inaccurate or that there are other systematic problems in the measurements. One possible problem with the calculations is that the vial walls may be thicker than used in the calculations, especially the bottom of the vials and possibly the bulge in the neck of the vials has a larger effect than expected. Nonetheless the inclusion of the p_{wall} correction in the NPL measurements reduces the discrepancies between the two techniques by nearly a factor of two. The source of the remaining discrepancies is of considerable interest but not yet understood.

TABLE III. Calculated wall-correction factors for NPL vials, other conditions as in Table II. The last column gives p_{air}, the calculated correction for the effect of a gas bubble filling the upper cylinder of the NPL vial. The 1 s.d. statistical uncertainties in the last digit are shown in brackets. The uncertainty in p_{air} reflects the final uncertainty in the product $p_{air}p_{wall}$.

Beam	TPR_{10}^{20}	p_{wall} (no air)	p_{air}
^{60}Co	0.58	0.9977(5)	0.9992(5)
4 MV	0.624	0.9954(8)	0.9997(7)
6 MV	0.667	0.9938(9)	0.9983(7)
10 MV	0.731	0.9928(11)	0.9985(6)
15 MV	0.761	0.9898(7)	0.9980(8)
24 MV	0.804	0.9883(6)	0.9974(6)

D. Kwa and Kornelsen experiment

Figure 7 shows a comparison of the Kwa and Kornelsen's measured[10] and our calculated ratio of Fricke doses at the same point in Fricke vials made of pyrex and polystyrene. The comparison is very similar to that done for the NRC experiment described above in Sec. V B 2. The measurements and calculations are in good agreement although the measurement uncertainties are much larger in this case than in the NRC measurements. These results have been discussed in detail elsewhere.[9]

E. Measurements around vials

Figure 8 presents a comparison of measured and calculated dose increases in a 20-MV photon beam near the

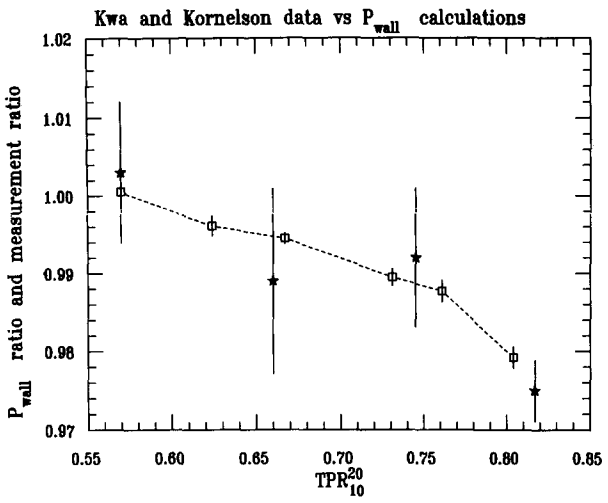

FIG. 7. Comparison of calculated (squares) and "measured" ratios of doses to Fricke solution in Kwa and Kornelsen's vials of pyrex and polystyrene.[10] The calculated values are just the ratio of p_{wall} calculated for the pyrex vials divided by that for the polystyrene vials.

standard coin shaped NRC Fricke detector modelled with pyrex walls (which, as mentioned above, is equivalent to fused quartz in the calculations). The measurements were made with a diode detector with dimensions of about 1 mm (see Sec. IV B) and thus represent an integral of the dose in a region.

The dose measured immediately behind the Fricke vial (not shown) displays an increase of about 0.2% except directly behind the cylindrical walls where a 3.5% decrease occurred and outside the vial radius where up to a 1.2% increase in the dose was observed. Calculations predicted a small decrease in the dose immediately behind the vial (0.5%±0.2%) and accurately predicted the decrease in the region immediately behind the side wall of the vial (3.4%±0.7%).

Panel (a) of Fig. 8 shows that the measured and calculated backscatter from the flat wall of the Fricke vial plays a substantial role, leading to a 3% increase in the dose in the first mm upstream of the vial wall but dropping fairly rapidly to less than 0.5% at 3 mm. This backscatter was measured and calculated to be constant over the entire front surface. This is an electron backscatter effect which disappears completely in the Monte Carlo calculations if all electron multiple scattering is turned off. The backscatter will also occur at the back wall inside the vial and increase the Fricke detector response. Taking into account just this backscatter in the 7.3-mm-thick NRC vial would imply roughly a 0.6% effect on the detector response (of a total calculated effect of 1.4% at this energy).

Panels (b) and (c) of Fig. 8 show the measured and calculated dose increases at various radii outside the curved walls of the vial as a function of the distance from the front face. Panel (b) shows the data for the region closest to the vial. The calculations are in reasonable agreement with the measurements and exhibit the same, somewhat unusual, behavior of increasing near the front of the vial and then falling off. The dose near the side wall is

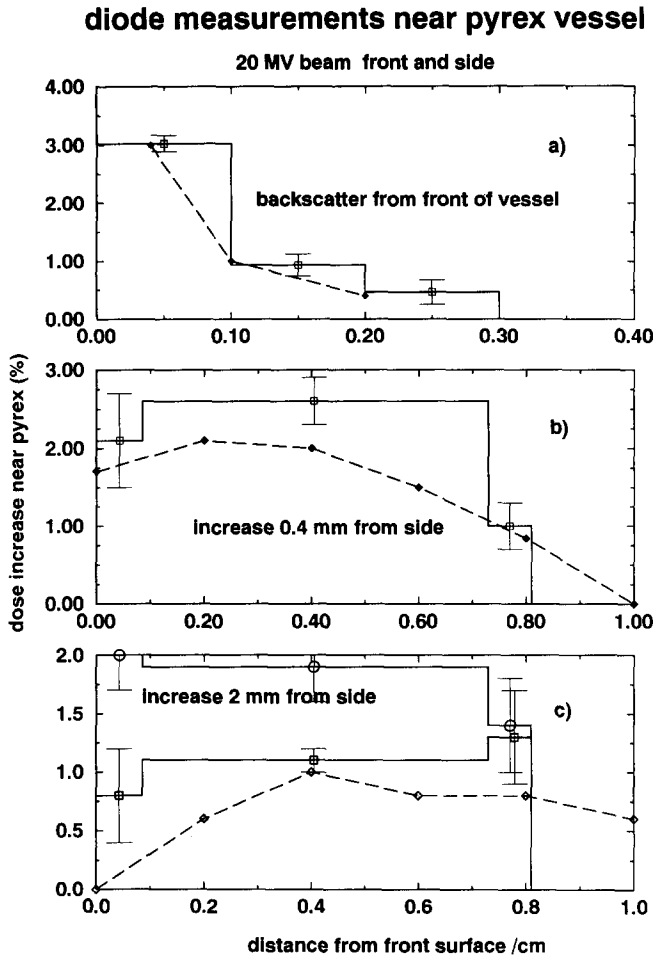

FIG. 8. Comparison of calculated and measured percentage increases in the dose to water measured near the standard NRC quartz-walled Fricke detectors (see Fig. 1) when irradiated at 7-cm depth in a 20-MV photon beam. The measured values are shown as diamonds joined by a dashed line and the calculated results are shown as histograms. Panel (a) shows the average dose increase at various distances upstream of the vessel. It is constant across the front of the vessel. Panels (b) and (c) show the percentage increase at various distances beside the curve surface of the vessel as a function of depth measured from the front face of the vessel. The calculations in panel (b) are for the dose in a ring 1 mm wide, immediately beside the vial wall and in panel (c) the calculations are for the dose in rings 1 to 2 mm (upper histogram) and 2 to 3 mm (lower histogram) from the side of the vial. The measured values were at 0.4 mm from the surface in panel (b) and 2 mm from the surface in panel (c). At a radial distance 4 mm from the side surface there was no measured increase in dose.

affected by three processes. The first is the increased multiple scattering from the quartz wall which tends to increase the dose downstream on either side of the wall. But even with all the electron multiple scattering turned off, the dose beside the wall at the back increases somewhat in the calculations because the increased density of the quartz compared to water causes more electrons to be set in motion. As well, very close to the wall, the effects of increased photon attenuation play a role near the back of the vial. Recall the 3.5% decrease directly behind the side wall. Thus in panel (b) we see a decrease near the vial wall at the back of the vial whereas further out from the wall the dose increases with depth because the effects of the in-

creased scattering upstream still dominate. Recall that in the scans behind the vial a 1.2% increase was measured outside the vial after the 3.5% decrease immediately behind the vial.

The calculated side-wall effects generally overestimate the measured effects although both the statistics of the calculations and the possible alignment uncertainties in the measurements are such that the discrepancies are not likely to be significant. It is also hard to utilize these results in a simple manner to estimate the overall effect of the side walls on the Fricke response for two reasons. First, in the interior there is a focusing effect which means the dose increase inside the wall will be more important than outside. Second, inside the vial, the scattered electrons will hit the back wall with an increased angle and hence there will be a synergistic effect which tends to increase the backscatter from the back wall. Ignoring both of these effects, a crude calculation based on the measured values outside the vials would suggest a 0.6% increase in the overall response because of the increased scatter from the side walls.

In summary, the measurements around the standard NRC vials show that the primary cause of the increased dose to the Fricke solution is from electron scattering effects from the back wall and the side walls and the calculations also indicate that the increased glass density plays a role near the side walls. In another set of calculations the walls were modeled as natural quartz which is chemically the same as fused quartz (SiO_2) but has a 20% greater density (2.65 g/cm^3). In this case the effects of the walls increased by 0.1% for low-energy beams and by up to 0.6% at high energies. This further emphasizes the important role of the density of the wall.

F. Extrapolation versus wall thickness

A possible experimental approach to determining the wall correction is to measure the response for additional wall thickness and extrapolate to zero wall thickness. This is an extremely difficult measurement to make accurately because the effects are so small. However, it is valuable to calculate the effects in this situation, first to demonstrate that the linear extrapolation technique does not work if using extra wall thickness and hence the difficult experiments are not useful, and secondly because it elucidates the mechanisms involved. Figure 9 presents the calculated dose to the Fricke solution in a ^{60}Co beam versus the front and side wall thickness. The dose is plotted relative to the dose with no wall present. Especially for the side wall it can be seen that the effect is nonlinear in the wall thickness. Thus in a ^{60}Co beam, unless much thinner walls than in the standard vials are used, the wall effect can not be determined by linear extrapolation of measurements made with extra wall thickness added. One interesting point to note is that although the overall wall correction is unity, it is made up of two components which cancel—an increase in dose due to the side wall and a decrease in dose due to the front wall.

Simple photon attenuation calculations suggest that in a ^{60}Co beam the front walls of the detector should reduce the dose in the Fricke solution by 0.55%, in reasonable agreement with the value shown in Fig. 9 as the ratio of the response with and without the front wall. However this agreement is fortuitous. If the electron transport is not included in the Monte Carlo calculation, the effect of the front and back wall is only a 0.27% reduction in dose, i.e., although the front wall attenuates the primary beam by 0.55%, the additional dose from photon scatter changes the net effect to 0.27%. Thus electron scatter effects play an important role even for the front and back walls where the attenuation appears to behave in a linear fashion. Most of this effect is electrons backscattering from the back wall. The effect of the side walls is almost entirely an electron scattering effect. It is reduced from the 0.6% effect seen in Fig. 9 to only 0.15% if electron transport is not included in the calculation.

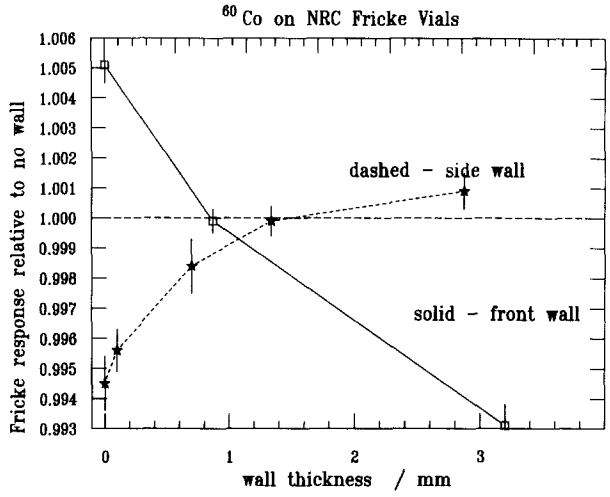

FIG. 9. Monte Carlo calculated response of Fricke solution in a standard NRC-like vial as the fused quartz wall thickness is varied in a ^{60}Co beam. Responses are shown relative to the response without a wall present. The other wall is held at its standard thickness in each case as one wall is varied. The standard front and back walls are 0.87 mm thick and the standard side wall is 1.34 mm thick. The front and back walls are varied at the same time.

VI. CONCLUSIONS

Monte Carlo calculations predict, and our high precision measurements confirm, that the walls of Fricke dosimeter vials play a significant role in Fricke dosimetry in photon beams. Counteracting effects in low-energy beams imply that the net correction in a ^{60}Co beam is negligible whereas it is as large as 2% in a 24-MV beam for the standard NRC vial with quartz walls. The effect can be made much smaller ($<0.2\%$ using PMMA walls) but in this case care must be taken to avoid storage effects in the Fricke solution.

Calculations and measurements demonstrate that the major source of these vial-wall effects is the increased multiple scattering from the relatively high-Z nuclei in the glass. Both the electron backscattering from the back wall of the vials and increased in-scatter from the side walls tend to increase the dose delivered to the Fricke solution. The increased density of material in the side walls also

leads to increased dose in the Fricke solution since more electrons are set in motion. At lower energies these increases are almost completely compensated for by photon attenuation and scattering effects and standard Burlin cavity theory effects.

These results directly affect the primary standards of absorbed dose both at NRC and at the PTB in Germany since both laboratories utilize glass-walled Fricke vials as part of their standard. NRC now includes calculated corrections for this effect, given the excellent agreement between the calculations and the experimental results. Measured corrections cannot be used directly since the measurements only give the ratio of correction factors, not the correction factors themselves. The effect on the PTB standard should be less because the calculated corrections are smaller for the NPL-like vials which are also used at the PTB. These results also directly affect the NPLs widely used Fricke dosimetry service which uses glass-walled chambers. Our results for plastic-walled vials imply that the extensive work by Mattsson *et al.*,[32,5] who used a PMMA walled vial, is not significantly affected by wall perturbations.

The comparison of the current calculations and measurements are sufficiently convincing that one might use the calculated corrections when glass-walled vials are needed for dosimetry services in which storage and transport are essential. This would introduce a beam quality dependence in the Fricke dose measurements. For use with primary standards it may be preferable to utilize plastic vials in order to minimize these wall effects and reduce the dependence on calculated corrections.

The results in Table I for the absorbed-dose conversion factor for converting the absorbed dose in Fricke to that in water show that this factor is roughly constant at 1.003 $\pm$0.001 for all beam energies and vial sizes studied in this work. This constancy is somewhat fortuitous since the detectors change from being mostly large cavity photon detectors in low-energy beams to being more small cavity electron detectors in high energy beams. This value is close to what was being used previously, but this represents the first time these values have been calculated accurately.

APPENDIX: DETAILS OF VIAL MODELS

A. NRC vials

The standard vials used for the NRC Fricke dosimetry service are made of fused quartz (ρ=2.2 g/cm^3). They are modeled as pyrex glass (ρ=2.23 g/cm^3) which, as mentioned in the text, is equivalent to using fused quartz in the calculation. The vials have a 2.861-cm inner diameter, 0.73-cm inner thickness, flat-wall thickness 0.087 cm and curved-wall thickness 0.134 cm. Calculations have also been done for vials with the same dimensions but made of polystyrene (ρ=1.06 g/cm^3), PMMA (ρ=1.19 gm/cm^3), and polyethelene (ρ=0.93 g/cm^3). The Fricke solution has a density of 1.023 g/cm^3. The vials were simulated with their flat faces perpendicular to the beam, i.e., parallel to the surface of the phantom.

For measurements done at NRC, a second series of vials was used with walls made of polyethylene. These were actually small bottles with screw on caps. They were modeled as having a 0.16-cm-thick bottom wall, a 0.12-cm side wall for 2.49 cm at which point the bottle narrowed to a neck which was 1.53 cm long with a wall thickness of 0.23 cm. The side wall and neck overlapped by 0.2 cm. The cap had 0.155-cm-thick walls which extended 0.80 cm down the side and attached to a 0.13-cm-thick top. The inner radius of the base of the bottle was 0.675 cm and the inner radius in the neck region was 0.41 cm. The bottle stood vertically with the midpoint of the beam striking it on the side wall, 2.15 cm above the base of the bottle. On occasion, small air bubbles remained inside the bottle after it was filled with Fricke solution. To see if this had any effect on the calculated results, in one of the geometries a 3-mm region of air was situated above the Fricke solution, replacing the Fricke solution. This is much greater than any actual air bubbles which were observed in practice but was used to give an upper limit on the effects of air bubbles.

B. NPL Vials

The vials used by the Fricke dosimetry service at NPL are made of pyrex-like glass and have been modeled as pyrex. They are not completely regular since they are individually flame sealed.[7] They have a gas bubble at the top of the vial. These vials are similar to some of those used at the PTB. The calculations do not include the effects of any air gaps or support mechanisms outside the vials which, in principle, must be accounted for.

The vials are basically vertical bottles which narrow towards the top in an irregular manner. However, they are modeled as two attached cylinders with a 0.07-cm-thick base and 0.05-cm-thick side walls. The lower cylinder is 3.07 cm long with an inner radius 0.55 cm. Calculations for two different models of the upper cylinder were done to encompass the variations between NPL and PTB vials as well as vial to vial variations. The upper cylinder is 2.00 cm long with an inner radius 0.35 or 0.25 cm, topped with a 0.05-cm-thick cap. The collar holding the two cylinders together is 0.05 cm thick. The center of the beam is modeled as passing through the middle of the side wall of the wide part of the vial. In one geometry the top cylinder was filled with air and in another option it was filled with Fricke solution. The results for the two different versions of the upper cylinder have been averaged because in all cases, no significant differences were found.

C. Kwa and Kornelsen vials

Calculations simulating the experiments of Kwa and Kornelsen have been described in detail elsewhere[9] but are included briefly here for completeness. In the simulations the vial was considered to be a long cylinder with its axis perpendicular to the beam. It has an inner diameter of 1.354 cm, a wall thickness of 0.10 cm and an inner length of 5.5 cm. This has the same cross sectional area, length

(in one case) and wall thickness as the square vials used by Kwa and Kornelsen. Walls of pyrex and polystyrene were simulated.

[a]Present address: NRC, Ottawa.

[1]ICRU Report 14, *Radiation Dosimetry: X-Rays and Gamma-Rays with Maximum Photon Energies Between 0.6 and 50 MeV* (ICRU, Washington, D.C., 1969).

[2]ICRU Report 35, *Radiation Dosimetry: Electron Beams with Energies between 1 and 50 MeV* (ICRU, Washington, D.C., 1984).

[3]ICRU Report 34, *The Dosimetry of Pulsed Radiation* (ICRU, Washington, D.C., 1984).

[4]AAPM TG-21, "A protocol for the determination of absorbed dose from high-energy photon and electron beams," Med. Phys. **10**, 741–771 (1983).

[5]O. Mattsson, K.-A. Johansson and H. Svensson, "Ferrous sulphate dosimeter for control of ionization chamber dosimetry of electron and ^{60}Co gamma beams," Acta Radiol. Oncol. **21**, 139–144 (1982).

[6]H. Svensson, C. Pettersson, and G. Hettinger, *Effects on Ferrous Sulphate Dosimeter Solution Stored in Small Polystyrene Cells* in Proc. Solid State and Chemical Radiation Dosimetry in Medicine and Biology, pp. 251–255 (IAEA, Vienna, 1967).

[7]S. C. Ellis, *The Dissemination of Absorbed Dose Standards by Chemical Dosimetry—Mechanism and Use of the Fricke Dosimeter,* NPL Report Rad. Sci. 30 (NPL, Teddington, 1974).

[8]T. E. Burlín and F. K. Chan, "The effect of the wall on the Fricke dosimeter," Int'l J. Appl. Rad. Isotop. **20**, 767–775 (1969).

[9]C.-M. Ma and A. E. Nahum, "Dose conversion and wall correction factors for Fricke dosimetry in high-energy photon beams: Analytical model and Monte Carlo calculations," Phys. Med. Biol. **38**, 93–114 (1993).

[10]W. Kwa and R. Kornelsen, "Comparison of ferrous sulphate (Fricke) and ionization dosimetry for high-energy photon and electron beams," Med. Phys. **17**, 602–606 (1990).

[11]W. R. Nelson, H. Hirayama, and D. W. O. Rogers, "The EGS4 Code System," Stanford Linear Accelerator Center Report SLAC-265 (Stanford Calif) (1985).

[12]C.-M. Ma, "Monte Carlo simulation of dosimeter response using transputers," London University (Institute of Cancer Research) PhD Thesis, ICR Physics Department, also available as Report ICR-PHYS-1/92 (1992).

[13]A. F. Bielajew, D. W. O. Rogers, and A. E. Nahum, "Monte Carlo simulation of ion chamber response to ^{60}Co–Resolution of anomalies associated with interfaces," Phys. Med. Biol. **30**, 419–428 (1985).

[14]D. W. O. Rogers, A. F. Bielajew, and A. E. Nahum, "Ion chamber response and A_{wall} correction factors in a ^{60}Co beam by Monte Carlo simulation," Phys. Med. Biol. **30**, 429–443 (1985).

[15]D. W. O. Rogers and A. F. Bielajew, "Wall attenuation and scatter corrections for ion chambers: Measurements versus calculations," Phys. Med. Biol. **35**, 1065–1078 (1990).

[16]A. F. Bielajew and D. W. O. Rogers, "PRESTA: The parameter reduced electron-step transport algorithm for electron Monte Carlo transport," Nucl. Inst. Meth. **B18**, 165–181 (1987).

[17]S. Duane, A. F. Bielajew, and D. W. O. Rogers, "Use of ICRU-37/NBS Collision Stopping Powers in the EGS4 System," NRCC Report PIRS-0177, Ottawa, March (1989).

[18]D. W. O. Rogers, G. M. Ewart, A. F. Bielajew and G. van Dyk, "Calculation of Electron Contamination in a ^{60}Co Therapy Beam," in *Proceedings of the IAEA International Symposium on Dosimetry in Radiotherapy* (IAEA, Vienna, 1988), Vol. 1, pp. 303–312.

[19]R. Mohan, C. Chui, and L. Lidofsky, "Energy and angular distributions of photons from medical linear accelerators," Med. Phys. **12**, 592–597 (1985).

[20]C. Malamut, D. W. O. Rogers, and A. F. Bielajew, "Calculation of water/air stopping-power ratios using EGS4 with explicit treatment of electron—positron differences," Med. Phys. **18**, 1222–1228 (1991).

[21]A. Kosunen and D. W. O. Rogers, "DDSPR: A Code for calculating photon beam depth-dose curves and stopping-power ratios for an arbitrary spectrum," National Research Council Canada Report PIRS-298 (1992).

[22]D. W. O. Rogers and A. F. Bielajew, "Monte Carlo techniques of electron and photon transport for radiation dosimetry," in *The Dosimetry of Ionizing Radiation*, Vol III, edited by K. R. Kase, B. E. Bjarngard, and F. H. Attix (Academic, New York, 1990), pp. 427–539.

[23]C. K. Ross, N. V. Klassen, K. R. Shortt, and G. D. Smith, "A Direct comparison of water calorimetry and Fricke dosimetry," Phys. Med. Biol. **34**, 23–42 (1989).

[24]K. R. Shortt, N. V. Klassen, C. K. Ross, and G. D. Smith, "Ferrous sulfate dosimetry and its role in establishing an absorbed dose to water standard for the National Research Council of Canada," in *Proceedings of NRC Workshop on Water Calorimetry, NRC Report 29637* (NRC, 1988) pp. 121–126.

[25]K. R. Shortt, C. K. Ross, A. F. Bielajew and D. W. O. Rogers, "Electron beam dose distributions near standard inhomogeneities," Phys. Med. Biol. **31**, 235–249 (1986).

[26]C.-M. Ma and A. E. Nahum, "Bragg-Gray theory and ion chamber dosimetry in photon beams," Phys. Med. Biol. **36**, 413–428.

[27]A. Kosunen and D. W. O. Rogers, "Beam quality specification for photon beam dosimetry," Med. Phys. (in press).

[28]J. E. Burns and J. W. G. Dale, *Conversion of Absorbed-Dose Calibration from Graphite into Water,* NPL Report RSA (EXT)7, (National Physical Laboratory, Teddington, UK, 1990).

[29]HPA, "Revised code of practice for the dosimetry of 2 to 35 MeV X-ray, and of caesium-137 and cobalt-60 gamma-ray beams," Phys. Med. Biol. **28**, 1097–1104 (1983).

[30]D. W. O. Rogers, "The advantages of absorbed-dose calibration factors," Med. Phys. **19**, 1227–1239 (1992).

[31]A. E. Nahum, D. I. Thwaites, and P. Andreo, "An analysis of the revised HPA dosimetry protocols," Phys. Med. Biol. **33**, 923–938 (1988).

[32]L. O. Mattsson, "Application of the water calorimeter, Fricke dosimeter and ionization chamber in clinical dosimetry," PhD Thesis, Univ. of Gothenburg (1984).